

# On the competition between delamination and shear failure in retrofitted concrete beams and related scale effects

A. Carpinteri, G. Lacidogna & M. Paggi

*Politecnico di Torino, Department of Structural and Geotechnical Engineering, Torino, Italy*

**ABSTRACT:** In this paper we deal with the most commonly reported failure modes related to interfacial stress concentrations at the FRP cut-off points, i.e. diagonal (shear) crack growth and FRP delamination. Depending on the mechanical properties of the tested beams, their geometry and size, a prevalence of a given failure mode to the other is very often experimentally observed. To analyze this failure mode competition, a combined analytical/numerical model is proposed for the determination of the critical loads required for the onset of delamination or shear failure. In this way, the experimentally detected failure modes observed in RC and FRC beams are reexamined and interpreted in this new framework.

## 1 INTRODUCTION

Structure rehabilitation is required whenever design mistakes, executive defects or unexpected loading conditions are assessed. In these cases, the use of a strengthening technique may be required in order to either increase the loading carrying capacity of the structure, or to reduce its deformations. The choice of the proper rehabilitation technique and the assessment of its performance and durability clearly represent outstanding research points. Among the different rehabilitation strategies, bonding of steel plates or FRP sheets on the concrete members is becoming increasingly popular (Hollaway & Leeming 1999).

In these situations, the main observed failure modes can be summarized as follows: (a) flexural failure by FRP yielding (Arduini et al. 1997), (b) flexural failure by concrete crushing in compression (Arduini et al. 1997), (c) shear failure (Ahmed et al. 2001), (d) concrete cover separation (David et al. 1993), (e) FRP delamination (Leung 2004a; Leung 2004b), and (f) intermediate crack induced debonding (Alaee & Karihaloo 2003; Wang 2006). Among them, shear failure, concrete cover separation and FRP delamination have been far more commonly revealed in experimental tests. In these cases, damage initiates near the FRP cut-off points due to the presence of a stress concentration or even a stress intensification. As a consequence, either a pure FRP delamination or a diagonal crack growth can occur. Moreover, in the latter case, depending on the amount of steel reinforcement and thickness of concrete cover, the diagonal crack may give rise to either shear failure, or concrete cover

separation. Therefore, since concrete cover separation occurs away from the FRP-concrete interface, this failure mode should be carefully distinguished from the pure FRP delamination. Therefore, it seems to be more appropriate to interpret failure modes (c) and (d) in the same framework.

As regards the mathematical models available in the Literature, most of them focus on the problem of delamination in steel plated and FRP strengthened beams (Smith & Teng 2002; Smith & Teng 2002b). Shearing and peeling stresses in the adhesive layer of a beam with a strengthening plate bonded to its soffit were determined in (Taljsten 1997; Malek et al. 1998; Ascione & Feo 2000; Smith & Teng 2001). The analysis of interface tangential and normal stresses in FRP retrofitted RC beams was also recently reexamined in (Rabinovitch & Frostig 2001; Rabinovitch 2004), along with a fracture mechanics model for the prediction of FRP delamination.

Comparatively, a little attention has been directed toward the analysis of shear crack growth and to the competition between FRP delamination and shear failure. The problem of size-scale effect is also an open issue (Maalej & Leong 2005). To deal with these problems, we propose a combined analytical/numerical model to describe the failure mode competition between FRP delamination and shear failure in reinforced concrete (RC) and fiber-reinforced concrete (FRC) beams. In this way, the experimentally detected failure modes are reexamined and interpreted in this new framework. As regards RC beams, we refer to the data on four-point bending tests

reported in (Ahmed et al. 2001), whereas the experimental results on FRC beams have been determined according to a new testing programme carried out in our laboratory.

## 2 ANALYTICAL MODEL

In this section, we consider the typical three-point bending and four-point bending tests carried out in the laboratories to assess the mechanical performance of retrofitted beams (see Fig. 1).

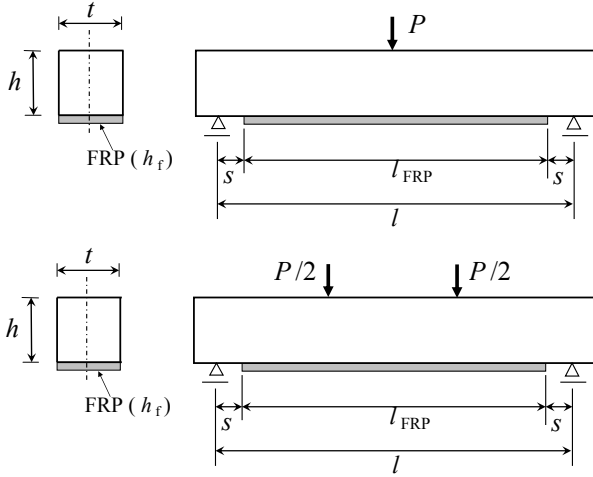


Figure 1: Schemes of three- and four-point bending tests.

### 2.1 Stress-singularities and generalized stress-intensity factors

According to Linear Elastic Fracture Mechanics, the FRP cut-off point can be a source of stress-singularities due to the mismatch in the elastic properties of concrete and FRP. The geometry of a plane elastostatic problem consisting of two dissimilar isotropic, homogeneous wedges of angles equal to  $\gamma_1 = \pi$  and  $\gamma_2 = \pi/2$  perfectly bonded along their interface is schematically shown in Figure 2.

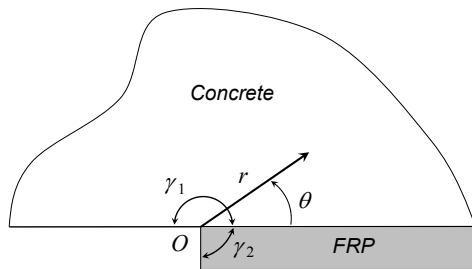


Figure 2: Scheme of the bi-material wedge composed of FRP and concrete.

In this general case, the singular components of the

stress field can be written as follows:

$$\sigma_{ij} = K^* r^{(\text{Re}\lambda-1)} S_{ij}(\theta), \quad (1)$$

where  $K^*$  is referred to as *generalized stress-intensity factor* (Carpinteri 1987). The parameter  $\lambda$  defines the order of the stress-singularity and can be obtained according to an asymptotic analysis of the stress field, see e.g. (Williams 1952; Bogy 1971; Carpinteri & Paggi 2005; Carpinteri & Paggi 2007) for similar applications.

According to this approach, the parameter  $\lambda$  is determined by solving a non-linear eigenvalue problem resulting from the imposition of the boundary conditions. In the present problem, they consist in the stress-free boundary conditions along the free edges, and in the continuity conditions of stresses and displacements along the bi-material interface. Since we are interested in the analysis of the singular terms of the stress field, we are concerned only with those values of  $\lambda$  which may lead to singularities. This fact, together with the condition of continuity of the displacement field at the vertex where regions meet, imply that we are seeking for eigenvalues in the range  $0 < \text{Re}\lambda < 1$ .

Function  $S_{ij}(\theta)$  in Eq. (1) is the eigenfunction of the problem and it locally describes the angular variation of the stress field near the singular point,  $O$ . It has to be remarked that, since both  $\lambda$  and  $S_{ij}(\theta)$  are determined according to the asymptotic analysis, they solely depend on the boundary conditions imposed in proximity of the singular point.

Moreover, from dimensional analysis arguments (Carpinteri 1987), it is possible to consider the following expression for the generalized stress-intensity factor:

$$K^* = \frac{Pl}{th^{1+\text{Re}\lambda}} f\left(\frac{h_f}{h}, \frac{l}{h}, \frac{l_{\text{FRP}}}{h}, \frac{E_f}{E_c}\right), \quad (2)$$

where function  $f$  depends on the boundary conditions far from the singular point and can be determined according to a FE analysis on the actual geometry of the tested specimen. For the sake of generality, this function depends on the relative thickness of the reinforcement compared to the beam depth,  $h_f/h$ , on the ratio between the span and the depth of the beam,  $l/h$ , on the length of the FRP sheet,  $l_{\text{FRP}}/h$ , and on the modular ratio between FRP and concrete,  $E_f/E_c$ . Parameters  $P$  and  $t$  denote, respectively, the applied load and the beam thickness.

The critical load corresponding to the onset of delamination can be determined by setting the generalized stress-intensity factor equal to the critical stress-intensity factor for the interface. This approach, well-established for the analysis of bonded joints (Reedy & Guess 1993; Qian & Akisanya 1999; Carpinteri &

Paggi 2006), yields to the following equation:

$$P_C^{\text{del}} = K_{C,\text{int}}^* \frac{th^{1+\text{Re}\lambda}}{l} \frac{1}{f}. \quad (3)$$

An analogous reasoning can be proposed for the analysis of the onset of shear failure, i.e. before the development of the crack-bridging effect due to steel reinforcement. In this case, we can postulate the existence of a small vertical crack into concrete at the FRP cut-off point simulating an initial defect. This crack may result in a sudden diagonal propagation leading to premature failure of the beam.

The stress field at the crack tip is again singular, but with the order of the singularity typical of a crack inside a homogeneous material (Carpinteri 1987; Bocca et al. 1990):

$$\sigma_{ij} = Kr^{-1/2} F_{ij}(\theta), \quad (4)$$

where function  $F$  locally describes the angular variation of the stress field near the crack tip. From dimensional analysis considerations, it is possible to write the following expression for the Mode I stress-intensity factor:

$$K_I = \frac{Pl}{th^{3/2}} g \left( \frac{a_0}{h}, \frac{h_f}{h}, \frac{l}{h}, \frac{l_{\text{FRP}}}{h}, \frac{E_f}{E_c} \right), \quad (5)$$

where function  $g$  depends again on the boundary conditions far from the singular point and can be determined according to a FE analysis on the actual geometry of the tested specimen. The additional parameter  $a_0$  with respect to FRP delamination denotes the initial crack length.

Crack propagation in this case takes place under Mixed Mode, although the Mode I stress-intensity factor is numerically prevailing. Under such assumptions, the critical load corresponding to the onset of shear crack propagation is reached when the Mode I stress-intensity factor equals the critical value of concrete. This condition yields to the following equation:

$$P_C^{\text{shear}} = K_{\text{IC}} \frac{th^{3/2}}{l} \frac{1}{g}. \quad (6)$$

### 2.2 Size-scale effects and failure modes competition

For a given tested beam, i.e., for a given beam geometry, the ratio between the critical loads for delamination and shear failure can be written as:

$$\frac{P_C^{\text{del}}}{P_C^{\text{shear}}} = \left( \frac{K_{C,\text{int}}^* g}{K_{\text{IC}} f} \right) h^{(\text{Re}\lambda-1/2)}, \quad (7)$$

which is a non-linear function of the beam depth. In addition, it is possible to recast Eqs. (3) and (6) in a

logarithmic form:

$$\log P_C^{\text{del}} = \log \left( \frac{tK_{C,\text{int}}^*}{lf} \right) + (1 + \text{Re}\lambda) \log h, \quad (8)$$

$$\log P_C^{\text{shear}} = \log \left( \frac{tK_{\text{IC}}}{lg} \right) + \frac{3}{2} \log h. \quad (9)$$

These equations are qualitatively plotted as functions of the beam depth in Figure 3. As expected, the higher the beam depth, for a given ratio  $l/h$ , the higher the critical load of failure. The intersection point between the two curves defines the critical beam size corresponding to the transition from pure delamination to shear failure. Moreover, since the real part of the eigenvalue  $\lambda$  is usually higher than 0.5, we expect a prevalence of shear failure in larger beams. In fact, if we consider  $E_f = 200$  GPa and  $E_c = 30$  MPa as the values representative of the Young's moduli of concrete and FRP, then the asymptotic analysis gives  $\lambda = 0.58$ .

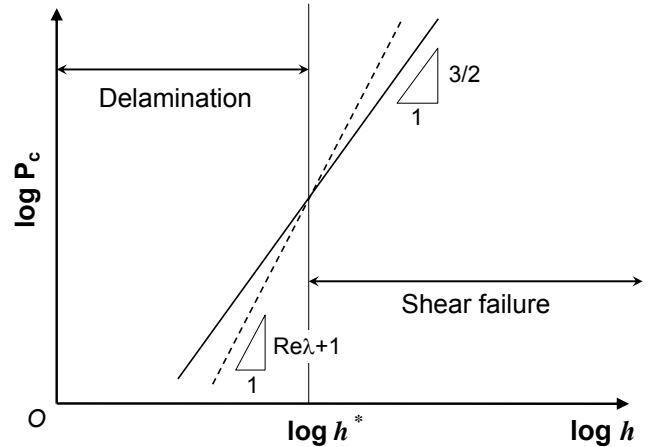


Figure 3: Competition between delamination and shear failure: dashed line corresponds to delamination, solid line corresponds to shear failure.

## 3 REINFORCED CONCRETE BEAMS

In this section we propose numerical simulations of shear failure and FRP delamination in FRP-retrofitted RC beams. Concerning the tested geometry, we refer to the extensive test programme carried out by Ahmed et al. (2001). More specifically, they tested a set of rectangular beams ( $h = 0.225$  m,  $l = 1.5$  m,  $t = 0.125$  m) under four point bending and considered different FRP lengths ( $l_{\text{FRP}} = 0.70$  m;  $0.65$  m;  $0.60$  m and  $0.55$  m). Independently of  $l_{\text{FRP}}$ , all the beams failed due to shear crack propagation originating from the FRP cut-off point. Numerical predictions and experimental results are shown and compared in the sequel.

### 3.1 Shear failure

The simulation of shear failure in RC beams can be performed according to different numerical strategies. For example, Gustraffson (1985) considered a FE formulation taking into account a softening cohesive law for concrete and truss elements connected by springs to the concrete blocks to model the presence of the reinforcement.

To avoid finite element computations, Jenq & Shah (1989) and So & Karihaloo (1993) proposed a semi-analytical model where the concrete contribution to shear strength was evaluated according to LEFM, and the effect of steel-concrete interaction was included using an empirical relationship.

In the present approach, we consider an initial crack length equal to  $a_0$  in correspondence of the FRP cut-off point. Simulation of crack growth is then performed using the FRANC2D finite element code (Wawrzynek & Ingraffea 1987). At each step, the stress-intensity factors are computed using the displacement correlation technique and the direction for crack propagation is determined according to maximum circumferential stress criterion. This approach permits to take into account the contribution of concrete to shear strength, as also done in the approximate model by Jenq & Shah (1989). Since the effect of reinforcement is not considered, the proposed method predicts an unstable crack growth, see e.g. Figure 4 for the case with  $l_{FRP} = 0.70$  m.

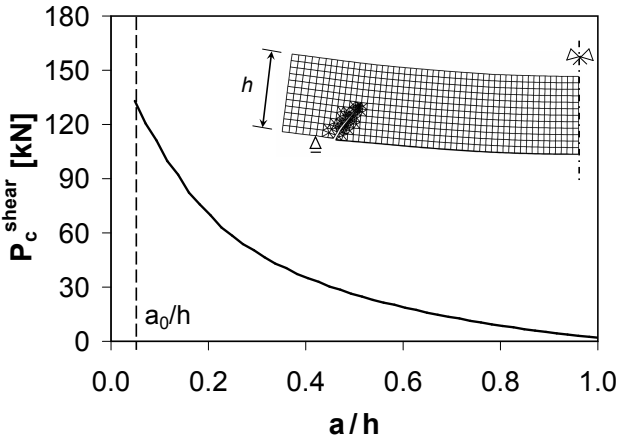


Figure 4: Critical load for shear failure vs. non-dimensional crack length.

The computed critical force corresponding to  $a_0$ , i.e. to the onset of diagonal failure, is shown in Figure 5 for different FRP lengths. Experimental results by Ahmed et al. (2001) are also reported in the same diagram. As expected, the good agreement between the numerical predictions and the experimental results demonstrate that this approach is suitable for the computation of the value of the critical force corresponding to the onset of crack propagation. Moreover, Fig-

ure 5 shows the shorter the FRP sheet, the lower the critical force.

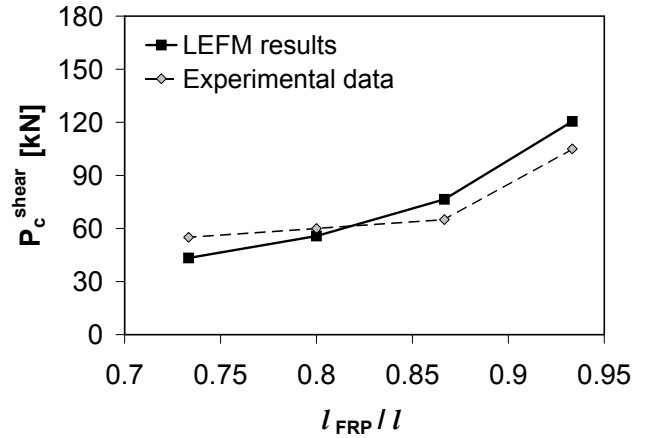


Figure 5: Critical load for shear failure vs. non-dimensional FRP length.

### 3.2 Delamination

The computation of the critical load required for delamination can be performed according to the analytical model illustrated in Section 2. In this case, the critical stress-intensity factor of the interface can be estimated as  $K_{C,int}^* \cong \sqrt{G_C E_a}$ , where  $G_C$  and  $E_a$  are, respectively, the interface fracture energy and the Young's modulus of the adhesive. These parameters can be determined either from experiments (Ferretti & Savoia 2003), or estimated according to the prescriptions reported in design codes and standards (ACI 440R-96 1996; fib Bulletin 2001; JCI 2003).

It is important to observe that the values of  $P_C^{del}$  computed for different FRP lengths, say  $l'_{FRP} < l_{FRP}$ , can also be obtained from the numerical simulation of the delamination process in a reference retrofitted beam with  $l'_{FRP} = l_{FRP}$ . In fact, considering an interface crack length equal to  $a$ , the debonded portion of the FRP sheet is stress-free. Under these conditions, the critical load for interface crack propagation,  $P_C^{del}(a)$ , corresponds to that for the onset of delamination in a retrofitted beam with a shorter reinforcement length, i.e.  $P_C^{del}(l_{FRP} - a)$ .

The progress of FRP delamination can be numerically simulated using the finite element method with a cohesive model for the description of the mechanical behavior of the interface. Cohesive models were introduced by Hillerborg et al. (1976) to the analysis of the nonlinear fracture process zones in quasi-brittle materials. Carpinteri firstly applied a cohesive formulation to the study of ductile-brittle transition and snap-back instability in concrete (Carpinteri 1985; Carpinteri et al. 1986; Carpinteri 1989). More recently, we have proposed the use of this approach for the analysis of snap-back instability during FRP delamination

(Carpinteri et al. 2006).

Numerical results for the beam with  $l_{FRP} = 0.70$  m are reported in Figure 6 in terms of the applied load,  $P$ , vs. the mid-span deflection,  $\delta$ . When the peak load is achieved, point (A), delamination takes place and, using the crack length as a driving parameter, we observe that both the external load and the mid-span deflection of the beam are progressively reduced up to point (B). After that, the progress of delamination requires an increase in the external load, tending asymptotically to the mechanical response of the undamaged RC beam without FRP. From the engineering point of view, this brittle mechanical response is particularly dangerous, since it corresponds to a severe snap-back instability. A deformed mesh showing the progress of delamination is also shown in Figure 7.

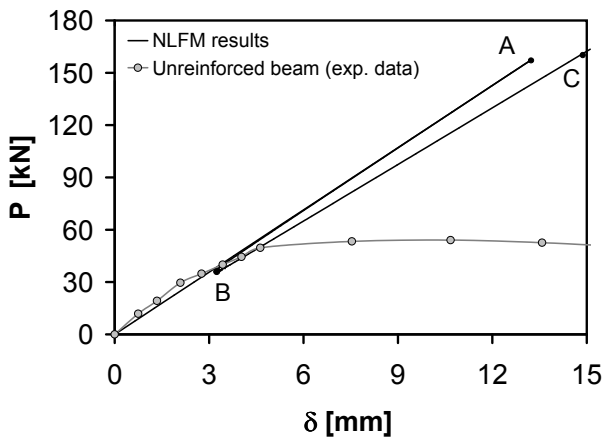


Figure 6: Load vs. non-dimensional deflection during delamination.

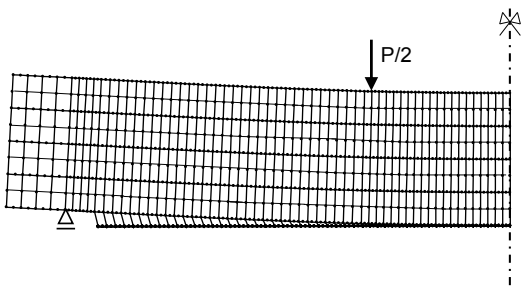


Figure 7: Deformed mesh showing delamination.

The structural response can be represented in terms of critical load vs. crack length or, equivalently, critical load vs. FRP length (see Fig. 8). During crack propagation, i.e. from (A) to (B), we have an unstable crack growth, since the external load is progressively reduced. An increase in the critical load is observed after point (B), i.e. for  $a/l_{FRP} \cong 0.8$ . In any case, for shorter FRP lengths, the actual failure load is certainly bounded by flexural or diagonal failures of the concrete beam (see e.g. Figures 6 and 8 where the criti-

cal load corresponding to flexural failure of the beam without FRP is reported for comparison).

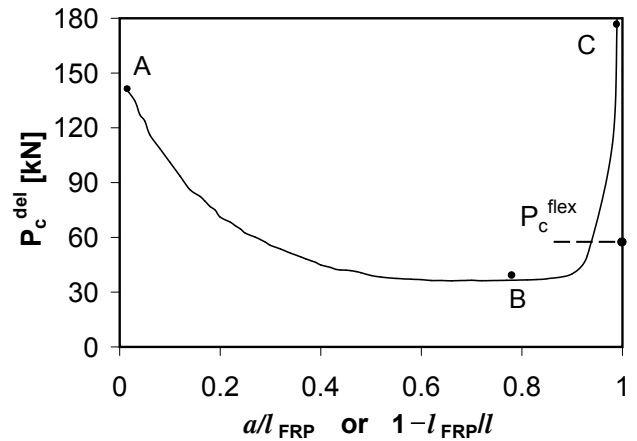


Figure 8: Critical load for delamination vs. non-dimensional crack advancement.  $P_C^{\text{flex}}$  is the ultimate load of the reference beam without retrofitting.

A comparison between Figures 4 and 8 shows that both the critical loads for shear failure and those for FRP delamination are decreasing functions of  $l_{FRP}$  in the usual range of FRP lengths. Moreover, for the case-studies herein analyzed, the critical loads for shear failure are less than those for FRP delamination. This numerical prediction is in agreement with the experimental findings by Ahmed et al. (2001), where the reinforced beams failed due to shear failure. According to Figure 3, a pure FRP delamination is expected for smaller beams.

These results permit to interpret the common experimental observation that shear failure and concrete ripping are the most frequently observed failure modes in RC beams tested in laboratory. FRP delamination is less frequent and should be ascribed to weak bonding properties.

#### 4 FIBER-REINFORCED CONCRETE BEAMS

In this section, we show some of the main results of an experimental programme on fiber-reinforced concrete beams (FRC) retrofitted with FRP. The tests have been conducted in the Laboratory of Materials and Fracture Mechanics of the Department of Structural and Geotechnical Engineering of the Politecnico di Torino.

In this respect, we notice that most of the current research studies on retrofitting techniques deal with standard RC members, whereas FRC beams are analyzed only in a few studies (Yin & Wu 2003). From the engineering point of view, FRC beams can be used for applications requiring high durability and the problem of retrofitting may arise when we are looking at another dimension of such members, namely, their

upgrading capability (Shah & Ouyang 1991; Wegian & Abdalla 2005).

In this programme, seven FRC beams have been tested under three-point bending up to failure under displacement control (see Fig. 9). The beams are made of high-strength concrete reinforced with standard steel fibers produced by Bekaert. These fibers have a length equal to 50 mm, a diameter equal to 0.50 mm, and a content of 40 kg/m<sup>3</sup>. The concrete Young's modulus is equal to 35 GPa, with a Poisson's ratio of 0.18. FRP sheets have a Young's modulus equal to 165 GPa, a tensile strength of 2300 MPa and a maximum tensile strain at failure of 1.8%. Concerning the geometrical parameters, we have  $l = 100$  cm,  $l_{FRP} = 70$  cm,  $h = t = 15$  cm,  $s = 7.5$  cm and  $h_f = 1.4$  mm.

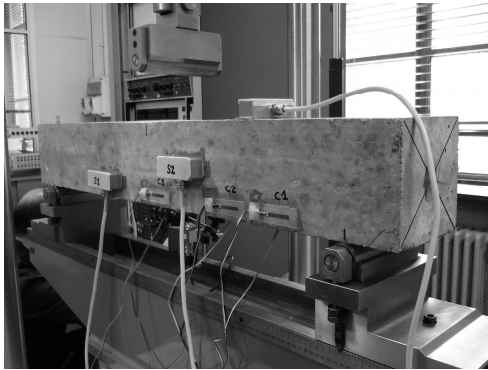


Figure 9: Photo of the testing apparatus.

Four retrofitted beams failed due to delamination (B2, B3, B5 and B6), two experienced shear failure (B1 and B4) and the remaining one was tested without FRP (B7) to establish the behavior of the unreinforced beam (see the test results shown in Figure 10). Photos of shear failure and FRP delamination are also shown, respectively, in Figures 11 and 12.

Experimental results indicate that mixing of steel-fibers affects the cracking behavior of concrete, giving rise to distributed crack patterns. The higher frequency of FRP delamination suggests that the failure mode changes from shear failure to pure FRP delamination, as compared to standard RC beams. This result is fully consistent with the analytical model in Section 2. In fact, the use of steel-fibers results into an increased concrete toughness as compared to regular concrete. As a consequence, higher values of  $K_{IC}$  correspond to the higher critical loads required for shear crack propagation (see Eq. (6)). Moreover, this confirms that the transition from FRP delamination to shear failure is expected for larger beams.

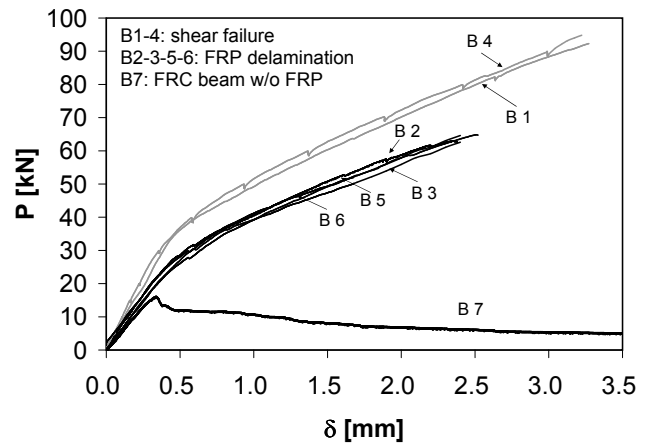


Figure 10: Results of the experimental tests: applied load vs. mid-span deflection.

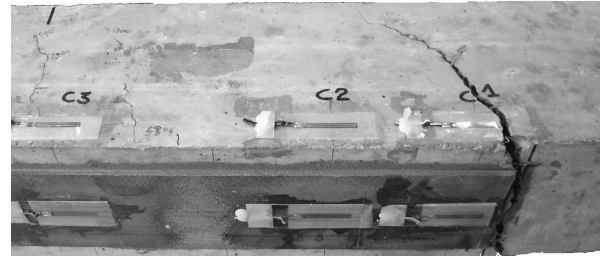


Figure 11: Photo of a failed beam due to shear crack growth.

## 5 CONCLUSIONS

In this paper we have proposed a combined analytical/numerical approach for the analysis of failure modes in concrete beams. Numerical predictions and experimental results show that shear failure and concrete ripping are more likely to occur in RC beams. In fact, for the analyzed case-studies, the critical load for the onset of shear crack growth is found to be lower than that corresponding to FRP delamination, independently of the reinforcement length. On the other hand, the results of the experimental programme on FRC beams show that in these cases FRP delamination is more frequent than shear failure. This different behavior as compared to RC beams has to be ascribed to the increased value of concrete fracture toughness due to the steel-fiber bridging effect.

Concerning the issue of stability of crack propagation, it has been shown that the process of FRP delamination leads to severe snap-back instabilities, thus resulting into a brittle mechanical response of the retrofitted concrete member. From the numerical point of view, it has been shown that the snap-back instability can be followed either under crack length control, or by computing the critical loads for delamination in correspondence of concrete beams with shorter and shorter FRP lengths. This numerical result



Figure 12: Photo of a failed beam due to FRP delamination.

gives also the possibility to experimentally follow the snap-back instability by testing concrete beams with different reinforcement lengths.

#### ACKNOWLEDGEMENTS

The financial support provided by the Italian Ministry of University and Research is gratefully acknowledged. The Authors would like to thank Mr. V. Di Vasto for the technical support provided during the experimental programme and Ing. R. Gottardo, Technical Manager of the D.L. Building Systems DEGUSSA Construction Chemicals Italia, for providing the FRP sheets used in the testing programme.

#### REFERENCES

- Ahmed, O., Van Gemert, D. & Vandewalle, L. 2001. Improved model for plate-end shear of CFRP strengthened RC beams. *Cement & Concrete Composites* 23: 3–19.
- Alaee, F. & Karihaloo, B. 2003. Fracture model for flexural failure of beams retrofitted with CARDIFRC. *ASCE Journal of Engineering Mechanics* 129: 1028–1038.
- Arduini, M., Di Tommaso, A. & Nanni, A. 1997. Brittle failure in FRP plate and sheet bonded beams. *ACI Structural Journal* 94: 363–370.
- Ascione, L. & Feo, L. 2000. Modeling of composite/concrete interface of RC beams strengthened with composite laminates. *Composites Part B: engineering* 31: 535–540.
- Bocca, P., Carpinteri, A. & Valente, S. 1990. Size effects in the mixed mode crack propagation: softening and snap-back analysis. *Engineering Fracture Mechanics* 35: 159–170.
- Bogy, D. 1971. Two edge-bonded elastic wedges of different materials and wedge angles under surface tractions. *ASME Journal of Applied Mechanics* 38: 377–386.
- Carpinteri, A. 1985. Interpretation of the Griffith instability as a bifurcation of the global equilibrium. In S. Shah (Ed.), *Application of Fracture Mechanics to Cementitious Composites (Proc. of a NATO Advanced Research Workshop, Evanston, USA, 1984)*, 287–316. Martinus Nijhoff Publishers, Dordrecht.
- Carpinteri, A. 1987. Stress-singularity and generalized fracture toughness at the vertex of re-entrant corners. *Engineering Fracture Mechanics* 26: 143–155.
- Carpinteri, A. 1989. Cusp catastrophe interpretation of fracture instability. *Journal of the Mechanics and Physics of Solids* 37: 567–582.
- Carpinteri, A., Lacidogna, G. & Paggi, M. 2006. Acoustic emission monitoring and numerical modelling of FRP delamination in RC beams with non-rectangular cross-section. *RILEM Materials & Structures, in press*. doi:10.1617/s11527-006-9162-4.
- Carpinteri, A. & Paggi, M. 2005. On the asymptotic stress field in angularly nonhomogeneous materials. *International Journal of Fracture* 135: 267–283.
- Carpinteri, A. & Paggi, M. 2006. Influence of the intermediate material on the singular stress field in tri-material junctions. *Materials Science* 42: 95–101.
- Carpinteri, A. & Paggi, M. 2007. Analytical study of the singularities arising at multi-material interfaces in 2D linear elastic problems. *Engineering Fracture Mechanics* 74: 59–74.
- Carpinteri, A., Di Tommaso, A. & Fanelli, M. 1986. Influence of material parameters and geometry on cohesive crack propagation. In F. Wittmann (Ed.), *Fracture Toughness and Fracture Energy of Concrete (Proc. of Int. Conf. on Fracture Mechanics of Concrete, Lausanne, Switzerland, 1985)*, 117–135. Elsevier, Amsterdam.
- David, E., Djelal, C. & Buyle-Bodin, F. 1993. Repair and strengthening of reinforced concrete beams using composite materials. Proceedings of the 2nd international PhD symposium in civil engineering, Budapest.
- Ferretti, D. & Savoia, M. 2003. Cracking evolution in R/C members strengthened by FRP-plates. *Engineering Fracture Mechanics* 70: 1069–1087.
- Gustafsson, P. 1985. Fracture mechanics studies of non-yielding materials like concrete. *Report TVBM-1007, Div. Build. Mater. Lund. Inst. Tech, Sweden*.
- Hillerborg, A., Modeer, M. & Petersson, P. 1976. Analysis of crack formation and crack growth

- in concrete by means of fracture mechanics and finite elements. *Cement and Concrete Research* 6: 773-782.
- Hollaway, L. & Leeming, M. 1999. *Strengthening of reinforced concrete structures*. Cambridge, England: Woodhead Publishing.
- Jenq, Y. & Shah, S. 1989. Shear resistance of reinforced concrete beams - a fracture mechanics approach. *Fracture Mechanics: Application to Concrete (Special Report ACI SP-118)*, eds. V.C. Li and Bazant, Z.P., Detroit 25: 327-358.
- Leung, C. 2004a. Delamination failure in concrete beams retrofitted with a bonded plate. *ASCE Journal of Materials in Civil Engineering* 13: 106-113.
- Leung, C. 2004b. Fracture mechanics of debonding failure in FRP-strengthened concrete beams. In V. Li, C. Leung, K. Willam, and S. Billington (Eds.), *Proceedings of the 5th International Conference on Fracture Mechanics of Concrete and Concrete Structures (FraMCoS-5)*, Vail, Colorado, USA, Volume 1, 41-52.
- Maalej, M. & Leong, K. 2005. Effect of beam size and FRP thickness on interfacial shear stress concentration and failure mode of FRP-strengthened beams. *Composites Science and Technology* 65: 1148-1158.
- Malek, A., Saadatmanesh, H., & Ehsani, M. 1998. Prediction of failure load of R/C beams strengthened with FRP plate due to stress concentration at the plate end. *ACI Structural Journal* 95: 142-152.
- ACI 440R-96 1996. State-of-the-art report on fiber reinforced plastic (FRP). Reinforcement for concrete structures. *American Concrete Institute, Committee 440, Michigan, USA*.
- fib Bulletin 2001. Design and use of externally bonded FRP reinforcement (FRP EBR) for reinforced concrete structures. Bulletin No. 14, prepared by subgroup EBR (Externally Bonded Reinforcement) of fib Task Group 9.3 FRP Reinforcement for Concrete Structures.
- JCI 2003. Technical report on retrofitting technology for concrete structures. Technical Committee on Retrofitting Technology for Concrete Structures.
- Qian, Z. & Akisanya, A. 1999. An investigation of the stress singularity near the free edge of scarf joints. *European Journal of Mechanics A/Solids* 18: 443-463.
- Rabinovitch, O. 2004. Fracture-mechanics failure criteria for RC beams strengthened with FRP strips-a simplified approach. *Composite Structures* 64: 479-492.
- Rabinovitch, O. & Frostig, Y. 2001. Delamination failure of RC beams strengthened with FRP strips-A closed form high-order and fracture mechanics approach. *ASCE Journal of Engineering Mechanics* 127: 852-861.
- Reedy, J. & Guess, T. 1993. Comparison of butt tensile strength data with interface corner stress intensity factor prediction. *International Journal of Solids and Structures* 30: 2929-2936.
- Shah, S. & Ouyang, C. 1991. Mechanical behavior of fiber-reinforced cement-based composites. *Journal of American Ceramics Society* 74: 2727-2738.
- Smith, S. & Teng, J. 2001. Interfacial stresses in plated beams. *Engineering Structures* 23: 857-871.
- Smith, S. & Teng, J. 2002. FRP-strengthened RC beams. I: review of debonding strength models. *Engineering Structures* 24: 385-395.
- Smith, S. & Teng, J. 2002b. FRP-strengthened RC beams. II: assessment of debonding strength models. *Engineering Structures* 24: 397-417.
- So, K. & Karihaloo, B. 1993. Shear capacity of longitudinally reinforced beams - a fracture mechanics approach. *ACI Journal* 78: 591-600.
- Taljsten, B. 1997. Strengthening of beams by plate bonding. *ASCE Journal of Materials in Civil Engineering* 9: 206-212.
- Wang, J. 2006. Cohesive zone model of intermediate crack-induced debonding of FRP-plated concrete beam. *International Journal of Solids and Structures* 43: 6630-6648.
- Wawrzynek, P. & Ingraffea, A. 1987. Interactive finite element analysis of fracture processes: an integrated approach. *Theoretical and Applied Fracture Mechanics* 8: 137-150.
- Wegian, F. & Abdalla, H. 2005. Shear capacity of concrete beams reinforced with fiber reinforced polymers. *Composite Structures* 71: 130-138.
- Williams, M. 1952. Stress singularities resulting from various boundary conditions in angular corners of plates in extension. *ASME Journal of Applied Mechanics* 74: 526-528.
- Yin, J. & Wu, Z. 2003. Structural performances of short steel-fiber reinforced concrete beams with externally bonded FRP sheets. *Construction and Building Materials* 17: 463-470.